第 43 卷 第 4 期/2023 年 2 月/光学学报 研究论文

光学学报

波长可调谐和异步双波长锁模掺铒光纤激光器

谢芷璇，邓樑旭，倪溢棉，曾浚壕，李艳*

广东技术师范大学光电工程学院，广东 广州 510665

摘要 利用激光诱导沉积法制备了碳纳米管可饱和吸收体，结合偏振控制器和保偏光纤产生的双折射滤波效应，在同一个环形掺铒光纤激光器中实现了波长可调谐，并获得了两种异步双波长锁模状态。通过调节泵浦功率和偏振控制器，获得了中心波长在1550 nm附近稳定可自启的锁模，波长可调谐范围为8.88 nm。同时，获得了两种异步双波长锁模状态，重复频率均约为49.9 MHz，脉冲重复频率差分别为1395 Hz和1089 Hz。

关键词 激光器；锁模；光纤激光器；碳纳米管；双波长；波长可调谐

中图分类号 TN248 **文献标志码** A **DOI**：10.3788/AOS221487

1 引 言

光纤激光器具有光束质量高、准直性强、结构简单紧凑和易于操作等优点，在光通信、非线性光学和生物医学等领域中具有广泛的应用[1-3]。常用的实现光纤激光器锁模的机制为被动锁模机制[4]，多种方法和技术被用于实现激光器的被动锁模，如非线性偏振旋转[5]、半导体可饱和吸收镜[6]、非线性光学环形镜[7]、石墨烯层[8]、碳纳米管[9]和新型二维材料[10]等。碳纳米管具有优越的非线性吸收特性，并具有制作方法简单、成本低的优点，故被广泛用于光纤激光器的被动锁模中，最终可获得高稳定性的超短脉冲。在碳纳米管被动锁模光纤激光器中，人们将制备好的碳纳米管/聚合物薄膜[11]或墙纸形态的碳纳米管薄膜[12]作为可饱和吸收体，实现了光纤激光器简单快速的搭建，但是该方法前期工作需要与材料制备配合紧密，且不利于可饱和吸收体的参数控制。激光诱导沉积法操作简单，且可通过控制激光功率和诱导时间来灵活地控制制备的可饱和吸收体的参数，为激光器领域内可饱和吸收体的制备提供了一种有效的手段。

与单一固定波长的激光器相比，波长可调谐或多波长锁模激光器在光通信、光纤传感和光谱学等诸多领域中具有更重要的应用[13-16]。迄今为止，人们研究了多种实现波长可调谐或多波长锁模激光器的方法。这些研究通过在激光器中加入滤波器件或装置实现波长可调谐或多波长锁模，如：马赫-增德尔干涉仪[17]、光纤光栅[18-20]、可调谐带通滤波器[21-22]等都被用于调节相应激光器的中心波长；腔内双折射效应[23-25]被用来实现激光器的波长可调谐或多波长锁模。与前者相比，后者不需要在腔内加入昂贵的滤波器件，故激光器结构更加简单，光谱可调范围也更加灵活。在现有研究中，一般只实现了波长可调谐或多波长锁模中的一种，且基本采用聚合物薄膜方式制备的可饱和吸收体来实现多波长被动锁模。关于通过灵活控制可饱和吸收体参数在同一个光纤激光器中实现波长可调谐和异步多波长锁模的研究还很少。

本文采用激光诱导沉积法制备了碳纳米管可饱和吸收体，利用腔内双折射效应，在同一掺铒光纤激光器中实现了波长可调谐和两种异步双波长锁模状态。在稳定可自启的锁模状态下，实验中通过调节偏振控制器，实现了中心波长从1545.52～1554.40 nm的连续可调。通过增加泵浦功率并改变腔内偏振态，实现了重复频率差分别为1395 Hz和1089 Hz的两种异步双波长锁模状态，中心波长分别为1533.03 nm/1544.45 nm和1545.36 nm/1555.53 nm，且两种异步双波长锁模状态之间可相互切换。

2 实验装置

2.1 可饱和吸收体的制作与参数测量

图1为可饱和吸收体的制作与参数测量实验装置示意图。首先，采用激光诱导沉积法[26]制作碳纳米管可饱和吸收体。然后，取适量碳纳米管浸泡在乙醇溶液中，加入适量表面活性剂（十二烷基苯磺酸钠），离心振荡使其均匀分散，并吸取少量溶液滴入离心管中。

收稿日期：2022-07-18；**修回日期**：2022-08-30；**录用日期**：2022-09-19；**网络首发日期**：2022-09-29

基金项目：国家自然科学基金（62105072）、广州市科技计划（202102020571）、广东大学生科技创新培育专项资金资助项目（pdjh2020b0343）、省级大学生创新创业训练计划（S202210588021）、广东技术师范大学人才引进科研启动项目（2021SDKYA169）

通信作者：*PE_liyan@gpnu.edu.cn

接着，将标准单模光纤跳线的一端浸入溶液中，在掺铒光纤激光器输出 5 mW 连续光条件下诱导 10 min 左右，实现光学沉积过程。最后，通过固定两根光纤跳线的方式对可饱和吸收体进行组装。

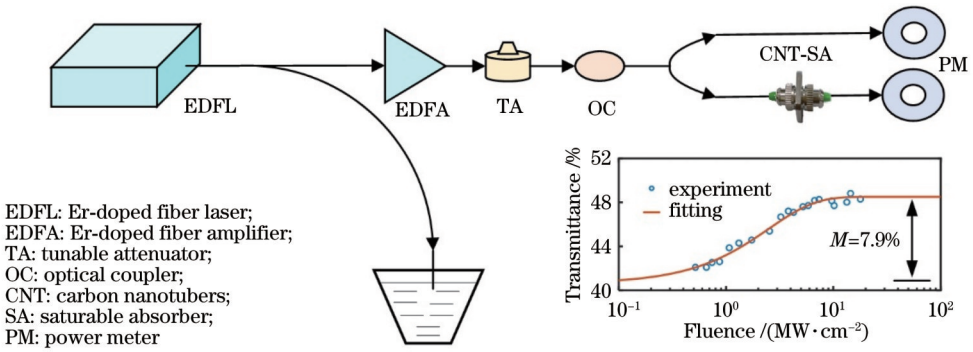

图 1　可饱和吸收体的制作与参数测量实验装置示意图（内插图为 CNT-SA 的非线性透射率曲线）

Fig. 1　Experimental setup for fabrication and parameter measurement of saturable absorber (inset is nonlinear transmittance curve of CNT-SA)

利用双探测器测量技术[27]对碳纳米管可饱和吸收体的透射率曲线进行测量，从而获得器件的非线性可饱和吸收特性参数。种子源由实验室已有的一台锁模掺铒光纤激光器和掺铒光纤放大器组成。种子源输出的 1550 nm 脉冲光经可调光衰减器后，利用一个分光比为 90∶10 的光纤耦合器对功率进行分割。90% 的光功率经过碳纳米管可饱和吸收体，并利用功率计对其进行测量，而另外 10% 的功率由另一个参考功率计进行测量。图 1 右下角的内插图中，圆形数据点为实验测得的碳纳米管可饱和吸收体的透射率数据。可饱和吸收模型[28]可表示为

$$T=1-M/(1+I/I_{\mathrm{sat}})-M_{\mathrm{n}}, \tag{1}$$

式中：T 是透射率；M 是调制深度；I 是输入光强度；I_{sat} 是饱和强度；M_{n} 是非饱和吸收率。采用该公式对数据进行拟合，得到器件的调制深度约为 7.9%。

2.2　多波长锁模掺铒光纤激光器结构

图 2 为搭建的多波长锁模掺铒光纤激光器的结构示意图。泵浦光由一个 980 nm 半导体激光器提供，通过一个 980/1550 nm 波分复用器耦合进环形腔中，腔内增益介质为一段 0.5 m 长的掺铒光纤。激光器采用制备的碳纳米管可饱和吸收体实现被动锁模。利用偏振不敏感的光纤隔离器来保证腔内激光的单向传输。光耦合器的输出比为 30%。腔内插入一段长度为 0.5 m 的保偏光纤，与前端的偏振控制器一起会产生双折射滤波效应。调节偏振控制器的旋转角度来改变腔内激光的偏振态，从而获得可调谐单波长和双波长锁模脉冲输出。

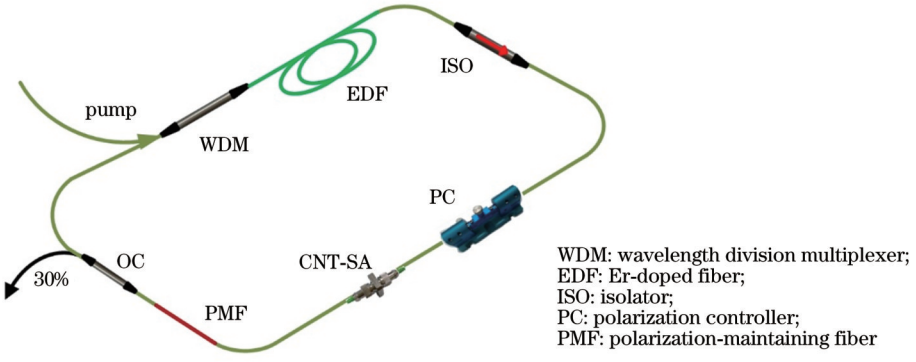

图 2　多波长锁模掺铒光纤激光器结构示意图

Fig. 2　Structural diagram of multi-wavelength mode-locked Er-doped fiber laser

实验中光纤激光器的输出参数由光谱仪（MS9710C）、光电探测器（DET08CFC/M）、数字示波器（N2831A）、自相关仪（FR-103XL）和射频频谱仪（DSA875-TG）获得。

3　实验结果与讨论

当泵浦功率增加到 30 mW 时，从耦合器输出端监测到中心波长在 1550 nm 附近的连续光。保持腔内偏振态不变，继续增加泵浦功率。当泵浦功率增加到 70 mW 时，可获得稳定可自启的单波长锁模脉冲。保

持其他参数不变，调节偏振控制器的旋转角度改变腔内光的偏振态，可获得波长可调谐的锁模脉冲输出。图 3(a)为测得的波长可调谐状态下的脉冲光谱变化。可以发现，光谱中心波长在 1545.52～1554.40 nm 范围内灵活可调：当光谱中心波长位于可调范围边缘时，光谱宽度较窄；当中心波长位于可调范围中间时，光谱宽度较宽。这主要是由相同泵浦功率下掺铒光纤(增益带宽通常为 1530～1560 nm)不同波段增益的变化引起的。同时，当中心波长小于 1548.11 nm 时，左侧 1532 nm 附近出现另一连续光，这与掺铒光纤在 1530 nm 附近具有增益峰吻合。

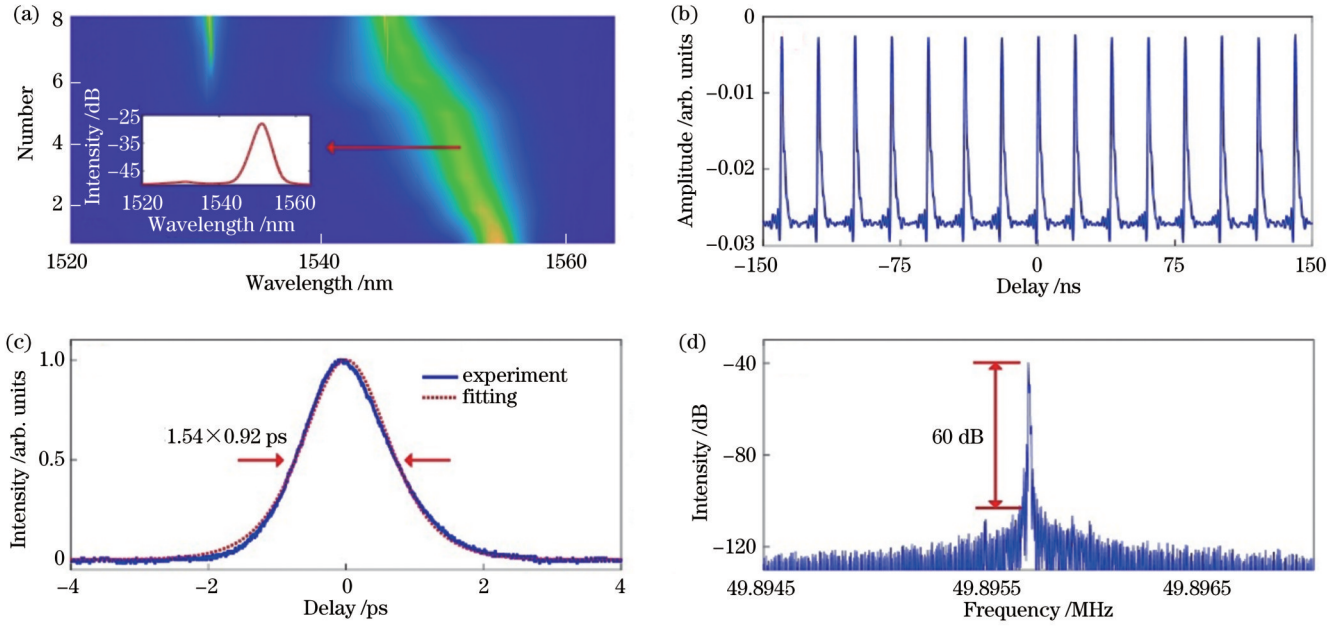

图 3　波长可调谐锁模状态下的脉冲输出特性。(a)光谱变化图(插图为 1551.18 nm 锁模时的光谱)；(b) 1551.18 nm 锁模时的示波器曲线；(c) 1551.18 nm 锁模时的自相关曲线；(d) 1551.18 nm 锁模时的射频频谱

Fig. 3　Pulse output characteristics under wavelength-tunable mode locking. (a) Spectral variation map (inset is mode-locking spectrum at 1551.18 nm); (b) oscilloscope curve at 1551.18 nm mode-locking; (c) autocorrelation curve at 1551.18 nm mode-locking; (d) radio frequency spectrum at 1551.18 nm mode-locking

在实验中，对可调范围中间位置处的脉冲参数进行了测量，光谱如图 3(a)中插图所示，中心波长和 3 dB 带宽分别为 1551.18 nm 和 2.8 nm。图 3(b)为对应脉冲的示波器轨迹图，呈稳定周期性输出。图 3(c)中实线为实验测得的对应脉冲的自相关曲线，在 sech^2 拟合(虚线)下，脉冲宽度约为 0.92 ps。计算可得，脉冲的时间带宽积为 0.321，由 sech^2 脉冲的最小时间带宽积约为 0.315 可知，脉冲接近变换极限。图 3(d)为对应脉冲的频谱图，实验测得脉冲的重复频率为 49.8957 MHz。该锁模状态下脉冲的平均输出功率约为 1.15 mW，单脉冲能量和脉冲峰值功率分别为 0.023 nJ 和 25 W。

继续增加泵浦功率到 140 mW，同时调节腔内偏振态，可获得异步双波长锁模脉冲，记为 Pulse 1。图 4(a)为中心波长分别在 1533.03 nm 和 1544.45 nm 时的双波长光谱，对应的光谱 3 dB 带宽分别为 0.85 nm 和 3.02 nm。此时，示波器上出现两个周期性扫描的梳齿，表明激光腔内存在两路群速度不同的孤子脉冲。图 4(b)为抓取的某时刻示波器轨迹图，脉冲周期约为 20 ns。实验测得的频谱数据如图 4(c)所示，两路孤子脉冲的重复频率分别约为 49.8971 MHz 和 49.8957 MHz，重复频率差为 1395 Hz。此时，激光器总的输出功率为 3.1 mW。仔细调节偏振控制器的旋转角度，可以对两路孤子的状态进行微调，实现部分脉冲能量从一路孤子到另一路孤子的转移。同时，两个中心波长位置处光谱的 3 dB 带宽也会发生相应变化。

保持泵浦功率 140 mW 不变，随着偏振控制器旋转角度的变化，将获得一种新的异步双波长锁模状态，记为 Pulse 2。图 4(d)为新的异步双波长锁模状态下的输出光谱，中心波长分别在 1545.36 nm 和 1555.53 nm，对应的光谱 3 dB 带宽分别为 2.49 nm 和 1.82 nm。在调节过程中，由于腔内偏振态和损耗发生了改变，故原来中心波长处于 1533.03 nm 的孤子消失，变成连续光。此时，另一路中心波长处于 1544.45 nm 的孤子对其的吸引作用也随之消失，该增益位置处的光谱中心波长由 1533.03 nm 左移到 1532.23 nm。同时，激光器在中心波长 1555.53 nm 处形成新的孤子，而原来中心波长为 1544.45 nm 的孤子由于长波段孤子的吸引，中心波长将右移至

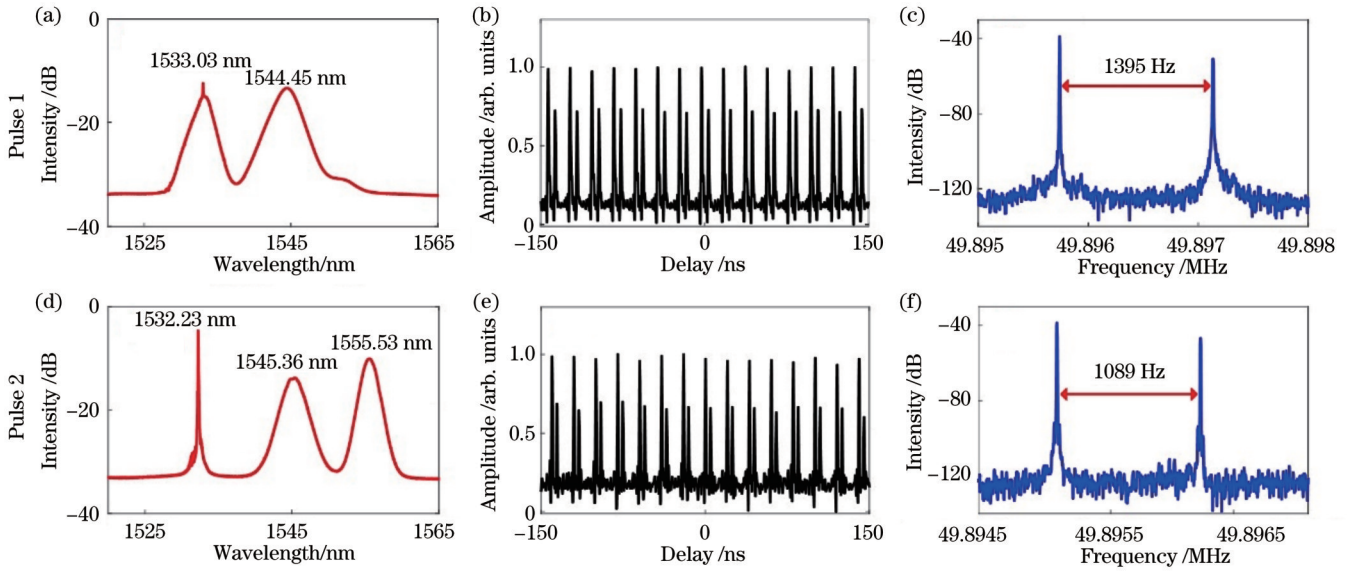

图 4 异步双波长锁模状态下的脉冲输出特性。(a)(d)光谱;(b)(e)示波器轨迹图;(c)(f)射频频谱

Fig. 4 Pulse output characteristics of asynchronous dual-wavelength mode locking. (a)(d) Spectra; (b)(e) are the oscilloscope traces; (c)(f) radio frequency traces

1545.36 nm。与第一种双波长状态相似,由于两路孤子具有不同的群速度,故此时示波器上依然会出现两个周期性扫描的梳齿。图 4(e)为该状态下抓取的某时刻示波器轨迹图。图 4(f)为测得的两路脉冲的频谱数据,其重复频率分别约为 49.8951 MHz 和 49.8962 MHz,重复频率差为 1089 Hz。此时,激光器总的输出功率基本保持不变。控制偏振控制器的旋转角度可实现上述两种异步双波长锁模状态的自由切换。

4 结 论

报道了一种基于碳纳米管可饱和吸收体的波长可调谐和异步双波长锁模掺铒光纤激光器,波长可调谐范围为 8.88 nm,两种异步双波长锁模状态下的重复频率差分别为 1395 Hz 和 1089 Hz。利用激光诱导沉积法制备的碳纳米管可饱和吸收体实现了两种异步双波长锁模脉冲输出,并在同一个激光器中获得了波长可调谐的锁模状态,研究结果在快速和多场景切换等光谱测量实际应用中具有重要价值。

参 考 文 献

[1] Keller U. Recent developments in compact ultrafast lasers[J]. Nature, 2003, 424(6950): 831-838.

[2] Evans C L, Xie X S. Coherent anti-Stokes Raman scattering microscopy: chemical imaging for biology and medicine[J]. Annual Review of Analytical Chemistry, 2008, 1: 883-909.

[3] Muñoz-Marco H, Abreu-Afonso J, Sardiello G, et al. Theoretical and experimental comprehensive study of GHz-range passively mode-locked fiber lasers[J]. Applied Optics, 2020, 59(23): 6817-6827.

[4] 董自凯, 宋晏蓉. 光纤激光器被动锁模技术研究进展[J]. 中国激光, 2021, 48(5): 0501006.
Dong Z K, Song Y R. Research progress of mode-locked fiber lasers based on saturable absorbers[J]. Chinese Journal of Lasers, 2021, 48(5): 0501006.

[5] 周飞, 周雪芳, 忻伶怡, 等. 基于NPR效应的可调谐多波长被动锁模光纤激光器[J]. 光电子·激光, 2021, 32(9): 919-926.
Zhou F, Zhou X F, Xin L Y, et al. A tunable multi-wavelength mode-locked fiber laser based on NPR effect[J]. Journal of Optoelectronics·Laser, 2021, 32(9): 919-926.

[6] Gomes L A, Orsila L, Jouhti T, et al. Picosecond SESAM-based ytterbium mode-locked fiber lasers[J]. IEEE Journal of Selected Topics in Quantum Electronics, 2004, 10(1): 129-136.

[7] Li Y, Quan M R, Tian J J, et al. Tunable multiwavelength erbium-doped fiber laser based on nonlinear optical loop mirror and birefringence fiber filter[J]. Applied Physics B, 2015, 119(2): 363-370.

[8] Fu B, Li J, Cao Z, et al. Bound states of solitons in a harmonic graphene-mode-locked fiber laser[J]. Photonics Research, 2019, 7(2): 116-120.

[9] 宋秋艳, 陈根祥, 谭晓琳, 等. 基于单壁碳纳米管的多波长被动锁模激光器[J]. 中国激光, 2014, 41(1): 0102002.
Song Q Y, Chen G X, Tan X L, et al. Multi-wavelength passively mode-locked laser based on single-walled carbon nanotube[J]. Chinese Journal of Lasers, 2014, 41(1): 0102002.

[10] Xu W X, Guo P L, Li X H, et al. Sheet-structured bismuthene for near-infrared dual-wavelength harmonic mode-locking[J]. Nanotechnology, 2020, 31(22): 225209.

[11] Guo J J, Ding Y H, Xiao X S, et al. Multiplexed static FBG strain sensors by dual-comb spectroscopy with a free running fiber laser[J]. Optics Express, 2018, 26(13): 16147-16154.

[12] Li X H, Wang Y G, Wang Y S, et al. Wavelength-switchable and wavelength-tunable all-normal-dispersion mode-locked Yb-doped fiber laser based on single-walled carbon nanotube wall paper absorber[J]. IEEE Photonics Journal, 2012, 4(1): 234-241.

[13] Talaverano L, Abad S, Jarabo S, et al. Multiwavelength fiber laser sources with Bragg-grating sensor multiplexing capability [J]. Journal of Lightwave Technology, 2001, 19(4): 553-558.

[14] Zhang A L, Liu H L, Demokan M S, et al. Stable and broad bandwidth multiwavelength fiber ring laser incorporating a highly nonlinear photonic crystal fiber[J]. IEEE Photonics Technology Letters, 2005, 17(12): 2535-2537.

[15] Liao R Y, Song Y J, Liu W, et al. Dual-comb spectroscopy with a single free-running thulium-doped fiber laser[J]. Optics

Express, 2018, 26(8): 11046-11054.
[16] 杨昌喜, 赵康俊, 曹博, 等. 单腔双光梳锁模光纤激光器及其应用研究进展[J]. 中国激光, 2021, 48(15): 1501001.
Yang C X, Zhao K J, Cao B, et al. Recent progress of single-cavity dual-comb mode-locked fiber lasers and their applications [J]. Chinese Journal of Lasers, 2021, 48(15): 1501001.
[17] Yin G L, Wang X Z, Bao X Y. Effect of beam waists on performance of the tunable fiber laser based on in-line two-taper Mach-Zehnder interferometer filter[J]. Applied Optics, 2011, 50 (29): 5714-5720.
[18] Litago I A, Leandro D, Quintela M Á, et al. Tunable SESAM-based mode-locked soliton fiber laser in linear cavity by axial-strain applied to an FBG[J]. Journal of Lightwave Technology, 2017, 35(23): 5003-5009.
[19] Liu X M, Han D D, Sun Z P, et al. Versatile multi-wavelength ultrafast fiber laser mode-locked by carbon nanotubes[J]. Scientific Reports, 2013, 3: 2718.
[20] 韩冬冬, 张佳月, 高琼, 等. 可切换多波长全光纤被动锁模光纤激光器[J]. 光学学报, 2021, 41(5): 0506002.
Han D D, Zhang J Y, Gao Q, et al. Switchable multi-wavelength passively mode-locked all-fiber lasers[J]. Acta Optica Sinica, 2021, 41(5): 0506002.
[21] Sun Z P, Popa D, Hasan T, et al. A stable, wideband tunable, near transform-limited, graphene-mode-locked, ultrafast laser [J]. Nano Research, 2010, 3(9): 653-660.
[22] 游关红, 彭万敬, 邹辉. 基于光学滤波器的扫频光纤激光器研究进展[J]. 激光与光电子学进展, 2021, 58(1): 0100006.
You G H, Peng W J, Zou H. Research progress of frequency-swept fiber lasers based on optical filter[J]. Laser & Optoelectronics Progress, 2021, 58(1): 0100006.
[23] Ozeki Y, Tashiro D. Fast wavelength-tunable picosecond pulses from a passively mode-locked Er fiber laser using a galvanometer-driven intracavity filter[J]. Optics Express, 2015, 23(12): 15186-15194.
[24] Huang S S, Wang Y G, Yan P G, et al. Tunable and switchable multi-wavelength dissipative soliton generation in a graphene oxide mode-locked Yb-doped fiber laser[J]. Optics Express, 2014, 22(10): 11417-11426.
[25] Zhang H, Tang D Y, Wu X, et al. Multi-wavelength dissipative soliton operation of an erbium-doped fiber laser[J]. Optics Express, 2009, 17(15): 12692-12697.
[26] Martinez A, Fuse K, Xu B, et al. Optical deposition of graphene and carbon nanotubes in a fiber ferrule for passive mode -locked lasing[J]. Optics Express, 2010, 18(22): 23054-23061.
[27] Fu B, Zhang C H, Wang P, et al. Nonlinear optical properties of Ag nanoplates plasmon resonance and applications in ultrafast photonics[J]. Journal of Lightwave Technology, 2021, 39(7): 2084-2090.
[28] Garmire E. Resonant optical nonlinearities in semiconductors[J]. IEEE Journal of Selected Topics in Quantum Electronics, 2000, 6(6): 1094-1110.

Wavelength-Tunable and Asynchronous Dual-Wavelength Mode-Locked Er-Doped Fiber Laser

Xie Zhixuan, Deng Liangxu, Ni Yimian, Zeng Junhao, Li Yan*

School of Optoelectronic Engineering, Guangdong Polytechnic Normal University, Guangzhou 510665, *Guangdong, China*

Abstract

Objective Wavelength-tunable and multi-wavelength ultrafast lasers, which can generate pulse trains at different center wavelengths, are applied widely in optical communication, sensing, and spectroscopy. In relevant research, different wavelength selection components, such as Mach-Zehnder interferometer filter, fiber Bragg grating and tunable filter, or birefringence-induced filtering (BRIF) effect are utilized for optical filtering. Compared with the former, the latter does not need to add expensive filter devices in the cavity. Additionally, the latter can also flexibly control the spectral spacing by adjusting the fiber length. Carbon nanotubes (CNTs), which can exhibit broad operation bandwidth at different spectral windows, are hotspots for multi-wavelength pulse generation. In current wavelength-tunable or multi-wavelength passive mode-locking fiber lasers based on CNT saturable absorber (SA), the SA is usually made by CNT/polyimide composite film, which is conducive to the simple and rapid construction of fiber lasers. However, compared with the laser-induced deposition method, this method requires close cooperation with material preparation, without benefiting the parameter controlling. Therefore, a wavelength-tunable and asynchronous dual-wavelength mode-locked Er-doped fiber laser based on CNT-SA obtained by the laser-induced deposition method is proposed. The results provide an approach to realize the wavelength-tunable and multi-wavelength mode-locked fiber laser simultaneously.

Methods The CNT-SA is obtained by the laser-induced deposition method. Firstly, CNTs are soaked in the alcohol solution with surfactant added. Secondly, the solution is transferred into a centrifugal tube after stirring. Thirdly, CNTs are deposited onto the core of a single-mode fiber by the optical power of 5 mW for ~10 min. Finally, the CNT-SA is assembled by fixing two single-mode fibers with an FC/APC ferrule. The wavelength-tunable and asynchronous dual-wavelength mode-locked fiber laser is passively mode-locked by the CNT-SA. A length of ~0.5 m Er-doped fiber is played as the gain medium, which is excited by a 980 nm pump via a wavelength division multiplexer. A polarization-

independent isolator is employed to ensure laser unidirectional transmission. A polarization controller (PC) and a length of ~0.5 m polarization-maintaining fiber (PMF) placed in the cavity are utilized for generating the BRIF effect. 30% of the energy is exported by a 30/70 optical coupler.

Results and Discussions A stable and self-starting mode-locking at the center wavelength around 1550 nm is obtained with the pump power of 70 mW. By the adjustment of the PC, the central wavelength can be tuned continuously in a range from 1545.52 nm to 1554.40 nm, with the spectral widths changed correspondingly. In wavelength-tunable operation, the superior characteristics of CNT-SA ensure stable mode-locking of pulses, and then the broad wavelength spacing caused by the PMF-based BRIF enables the pulses to get through it in a broad spectral range. For one typical single soliton mode-locked state of the fiber laser, the spectrum is centered at 1551.18 nm with a 3-dB spectral width of 2.8 nm. The estimated repetition frequency is 49.8957 MHz from the radio frequency (RF) spectrum. The corresponding pulse width is estimated to be 0.92 ps if a sech^2-shape pulse is assumed, with the time-bandwidth product of the pulses being 0.321, which is close to the transform limit. The output power, single pulse energy, and peak power of the output pulses are 1.15 mW, 0.023 nJ, and 25 W, respectively. Owing to the presence of birefringence and the cavity loss, the asynchronous dual-wavelength mode-locked states can be obtained when the pump power is increased to 140 mW and the state of the PC is adjusted. The central wavelengths of the two asynchronous pulse trains are located at 1533.03 nm and 1544.45 nm, respectively, with the 3-dB spectral width being 0.85 nm and 3.02 nm, respectively. The measured RF spectrum shows there are two main peaks at 49.8971 MHz and 49.8957 MHz, which indicates the repetition frequency difference of the two asynchronous pulse trains is 1395 Hz. Under the same pump power, another asynchronous dual-wavelength mode-locked state, with two central wavelengths located at 1545.36 nm and 1555.53 nm, respectively, can be obtained by adjusting the PC carefully. The repetition frequencies of the two asynchronous pulse trains are about 49.8962 MHz and 49.8951 MHz, respectively, with a repetition frequency difference of 1089 Hz. The two asynchronous dual-wavelength mode-locked states are switchable by controlling the PC settings.

Conclusions In this paper, wavelength-tunable and two asynchronous dual-wavelength mode-locking states are achieved in an Er-doped fiber ring laser, based on the birefringence filtering effect generated by PC and PMF, through a CNT-SA prepared by the laser-induced deposition method. By adjusting the pump power and PC, it obtains a stable and self-starting mode-locking at the center wavelength of around 1550 nm with a wavelength-tunable range of 8.88 nm. Moreover, two asynchronous dual-wavelength mode-locking states are obtained with repetition frequencies of around 49.9 MHz, and the repetition frequency differences are 1395 Hz and 1089 Hz, respectively. Multiple asynchronous dual-wavelength mode-locking states are realized with the assistance of the CNT-SA obtained by the laser-induced deposition method. The results are of great significance in fast spectral measurements and multi-scene switching applications.

Key words lasers; mode locking; fiber lasers; carbon nanotubes; dual-wavelength; tunable wavelength